Computational Journal of Mathematical and Statistical Sciences
x(x), 1–18
DOI:10.21608/cjmss.2025.380747.1175
https://cjmss.journals.ekb.eg/

Research article

Log-Inverse Gompertz Distribution: Properties and Application to Insurance and Soil Moisture Datasets

Abubakar Usman[1,*], **Gaber Sallam Salem Abdalla**[2], **Ehinomen Emmanuel Ehizojie** [3], **Yakubu Aliyu**[4]

[1] Department of Statistics, Faculty of Physical Sciences, Ahmadu Bello University, Zaria 234101, Nigeria; abubakarusman28@gmail.com.

[2] Department of Insurance and Risk Management, Faculty of Business, Imam Mohammed Ibn Saud Islamic University (IMSIU), Riyadh 11432, Saudi Arabia; jssabdullah@imamu.edu.sa.

[3] Department of Statistics, Faculty of Physical Sciences, Ahmadu Bello University, Zaria 234101, Nigeria; ehinomen116@gmail.com.

[4] Department of Statistics, Faculty of Physical Sciences, Ahmadu Bello University, Zaria 234101, Nigeria; yakubualiyu@abu.edu.ng.

* **Correspondence:** abubakarusman28@gmail.com

Abstract: Unit-bounded distributions are often used to mimic values that are strictly defined inside the interval (0, 1). Despite this, these distributions are more uncommon than those with semi-bounded support $(0, \infty)$. However, many real-life circumstances involve observations with a unit-bounded range, such as proportions, percentages, ratios, rates, and fractions. This study introduces the Log-Inverse Gompertz Distribution (LIGD), derived via a negative exponential transformation of the Inverse Gompertz distribution. The LIGD exhibits flexible density shapes (J, reversed-J, and left-skewed unimodal) and a strictly increasing hazard rate. The study examines statistical aspects and reliability measures such as survival, hazard, cumulative hazard, reversal hazard, quantile functions, median, skewness, kurtosis, and order statistics. The parameters of the proposed model were estimated using maximum likelihood estimation and maximum product of spacing, with a Monte Carlo simulation utilized to assess the efficacy of various estimating approaches. Finally, the proposed model's applicability is illustrated using two real-world data sets. A comparative analysis demonstrates that the proposed model outperforms many existing ones.

Keywords: Inverse Gompertz distribution, Goodness-of-fit tests, Reliability analysis, Simulation study, Unit-bounded distributions..

Mathematics Subject Classification: 60E05, 62E10, 62F10.

Received: 1 May 2025; Revised: 1 August 2025; Accepted: 4 August 2025; Online: 5 August 2025.

1. Introduction

The necessity to develop unit-bounded distributions, defined on the interval (0, 1), arises from the unique nature of data that falls within this range. These datasets are naturally bounded by 0 and 1, meaning that they cannot take values outside this range. Such data commonly represents proportions, ratios, percentages, probabilities, or rates, which are prevalent in numerous fields, including data science, economics, healthcare, risk analysis, and environmental studies. For instance, the proportion of total sales in an industry controlled by a particular Firm ranging from 0 (no market presence) to 1 (monopoly), the probability that a startup or business survives beyond a certain period, the percentage of income spent on food, the rate of people recovering from a disease, and the fraction of total income in an economy allocated to labour as opposed to capital. Thus, unit-bounded distributions are usually employed to model the behaviour of such random variables.

Recent literature has witnessed a significant rise in research focused on probability distributions confined to the unit interval, emphasizing the growing importance of these distributions in various fields of study. Some of these significant contributions can be found in literature including Korkmaz et al. [1], Mazucheli et al. [2], Altun and Cordeiro [3], Bashir et al. [4], Saboor et al. [5], Gemeay et al. [6], . Alghamdi et al. [7], Alsadat et al. [8], Haj et al. [9], and .Alyami et al. [10].

The Gompertz distribution (GD), known for its monotonically increasing hazard rate, has been adapted to analyze mortality data and mechanical failure patterns (Jha et al. [11]; Pandey et al. [12]). Eliwa et al. [13] proposed the Inverse Gompertz distribution (IGD) to model upside-down bathtub-shaped hazard rates, addressing limitations of the GD. In the past few years, significant contributions have been made to the study of the IGD. See, El-Morshedy et al. [14], Abdelhady et al. [15], Elshahhat et al. [16], Chaudhary et al. [17], Abd Ellatif and Abd Ellatif [18], Adegoke et al. [19], Baharith [20], Benkhelifa [21], Yadav and Kumar [22] and Al-Saqal et al. [23], among others. Other generalized distributions can be mentioned, such as gamma-normal distribution by Alzatreh et al. [24], a new two-parameter distribution by Suleiman et al. [25], a modified sine distribution by Uthumporn [26], Husain et al. [27], Sapkota et al. [28], Alsadat et al. [29], .Bantan et al. [30], among others.

In general, as mentioned earlier, the GD is flexible and often applied in various fields. However, the GD and IGD, as well as their extensions mentioned above, are useful for modelling certain types of data; they typically work best for semi-bounded data; thus, may struggle to model skewed and heavy-tailed unit-bounded data. The goal is to develop a novel unit-bounded distribution called Log-Inverse Gompertz distribution, which is an extension of the IGD by applying the logarithm of its random variable.

This paper is structured as follows: Section 2 details the formulation of the LIGD. Section 3 examines its key statistical properties and reliability measures. Parameter estimation methods are presented in Section 4, while Section 5 evaluates estimator performance through simulation studies. Section 6 demonstrates the model's practical application using two empirical datasets. The paper concludes with a discussion of findings in Section 7.

2. Log-Inverse Gompertz Distribution

By applying $X = e^{-Y}$, if rv $Y \sim \text{IGD}(\alpha, \beta)$, then the cumulative distribution function (cdf) is

$$G(y) = \exp\left[-\frac{\alpha}{\beta}\left(e^{\frac{\beta}{y}} - 1\right)\right], \quad y \in (0, \infty), \alpha, \beta > 0. \tag{2.1}$$

The cdf of LIGD is

$$F(x) = 1 - \exp\left[-\frac{\alpha}{\beta}\left(e^{-\frac{\beta}{\ln(x)}} - 1\right)\right], \tag{2.2}$$

and its probability density function (pdf) is

$$f(x; \alpha, \beta) = \frac{\alpha}{x(\ln(x))^2} \exp\left[-\frac{\alpha}{\beta}\left(e^{-\frac{\beta}{\ln(x)}} - 1\right) - \frac{\beta}{\ln(x)}\right], \quad x \in (0, 1) \tag{2.3}$$

where α and β are shape and scale parameters respectively. Unlike the IGD, the LIGD's pdf exhibits J-shaped and left-skewed unimodal forms as in Figure 1, broadening its applicability to unit-bounded data.

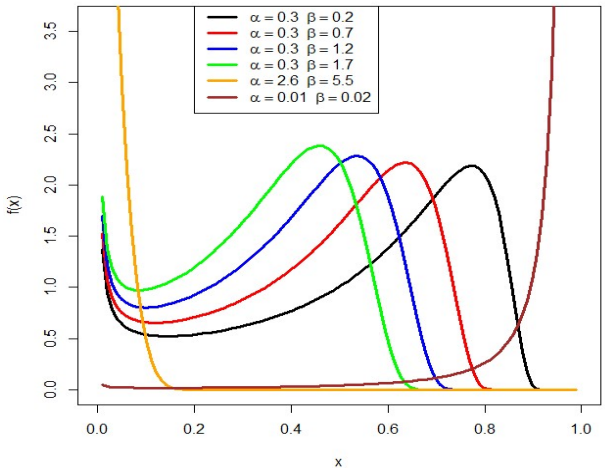

Figure 1. The pdf plots of LIGD.

3. Statistical Properties of LIGD

3.1. Reliability Measures

1. Survival function

$$S(x) = \exp\left[-\frac{\alpha}{\beta}\left(e^{-\frac{\beta}{\ln(x)}} - 1\right)\right] \tag{3.1}$$

2. Hazard rate function (hrf)

$$h(x) = \frac{\alpha e^{-\frac{\beta}{\ln(x)}}}{x(\ln(x))^2} \tag{3.2}$$

The behaviour of the hrf of LIGD is shown in Figure 2.

3. Reverse hazard function

$$r(x) = \frac{\alpha}{x\left(\ln\left(x\right)\right)^2} e^{-\frac{\beta}{\ln(x)}} \left[\left(e^{-\frac{\alpha}{\beta}\left(e^{-\frac{\beta}{\ln(x)}}-1\right)}\right)^{-1} - 1\right]^{-1} \tag{3.3}$$

4. Odd hazard function

$$\vartheta\left(x\right) = e^{\frac{\alpha}{\beta}\left(e^{-\frac{\beta}{\ln(x)}}-1\right)} - 1 \tag{3.4}$$

5. Cumulative hazard function

$$H(x) = \frac{\alpha}{\beta}\left(e^{-\frac{\beta}{\ln(x)}} - 1\right) \tag{3.5}$$

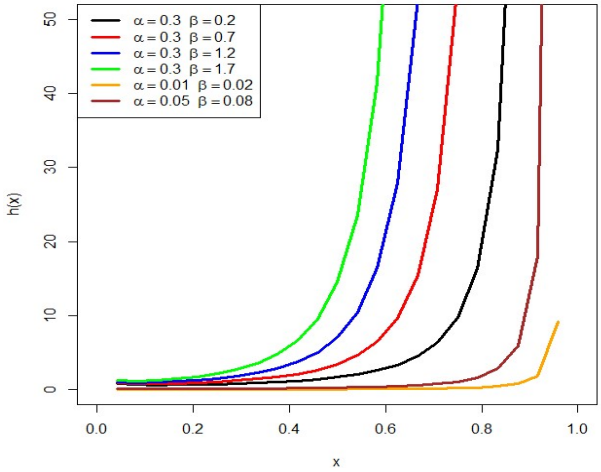

Figure 2. The hrf plots of LIGD.

Figure 2 shows that the LIGD's hrf exhibits monotonically increasing shapes. This suggests that the LIGD is suitable for modelling processes where the risk of an event increases over time, which is typical in aging-related failure processes or reliability models where failure becomes more likely as time progresses.

3.2. Quantile Function and Median

Quantile function

$$x_u = \exp\left[-\frac{\beta}{\ln\left(1 - \frac{\beta}{\alpha}\ln(1-u)\right)}\right], \quad 0 < u < 1; \tag{3.6}$$

setting $u = 0.5$ in Equation (3.6), the median of LIGD is given as

$$Med_x = \exp\left[-\frac{\beta}{\ln\left(1 - \frac{\beta}{\alpha}\ln(0.5)\right)}\right] \tag{3.7}$$

3.3. Skewness and Kurtosis

Quantile-based methodology for assessing the skewness and kurtosis of a distribution is particularly employed when its cdf has a closed form. Bowley [32] and Moor [33] proposed quantile-based measures of skewness and kurtosis for LIGD are respectively derived using Equation (3.7)

$$S_B = \frac{Q\left(\frac{3}{4}\right) - 2Q\left(\frac{2}{4}\right) + Q\left(\frac{1}{4}\right)}{Q\left(\frac{3}{4}\right) - Q\left(\frac{1}{4}\right)} \tag{3.8}$$

and

$$K_M = \frac{Q\left(\frac{7}{8}\right) - Q\left(\frac{5}{8}\right) + Q\left(\frac{3}{8}\right) - Q\left(\frac{1}{8}\right)}{Q\left(\frac{6}{8}\right) - Q\left(\frac{2}{8}\right)}; \tag{3.9}$$

Figure 3 displays the graphical representation of the median (Med_x), skewness (S_B) and kurtosis (K_M) measures of LIGD.

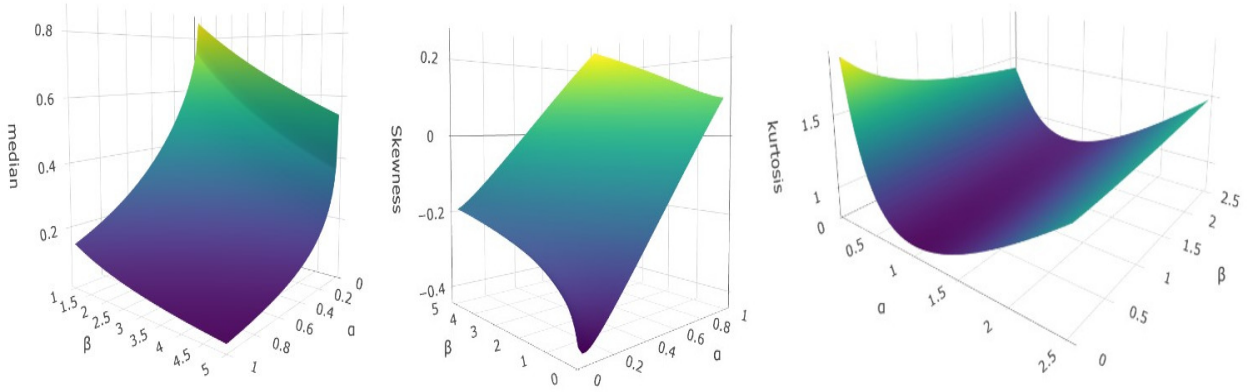

Figure 3. The 3D plot of the (Med_x), (S_B) and (K_M) of LIGD.

3.4. Order Statistics

Let $x_{(1)} \leq x_{(2)} \leq \ldots \leq x_{(n)}$, be the ordered statistic, then the pdf of the kth order statistic of LIGD is

$$f_{x_{(k)}}(x) = \frac{n!}{(k-1)!\,(n-k)!}\left(1 - e^{-\frac{\alpha}{\beta}\left(e^{-\frac{\beta}{\ln(x)}}-1\right)}\right)^{k-1}\left(e^{-\frac{\alpha}{\beta}\left(e^{-\frac{\beta}{\ln(x)}}-1\right)}\right)^{n-k}\frac{\alpha}{x\,(\ln(x))^2}e^{-\frac{\alpha}{\beta}\left(e^{-\frac{\beta}{\ln(x)}}-1\right)-\frac{\beta}{\ln(x)}} \tag{3.10}$$

4. Parameter Estimation

Here, the parameters of LIGD are estimated via two estimation techniques.

4.1. Maximum Likelihood Estimation (MLE)

Suppose a sample of n random samples $x_1, x_2, \ldots, x_n$ are drawn from the $LIGD(\alpha,\beta)$. The likelihood function is the product of the individual pdfs evaluated and given as

$$L(\alpha,\beta; x_1, x_2, ..., x_n) = \prod_{i=1}^{n} f(x_i;\alpha,\beta), \tag{4.1}$$

substituting Equation (2.3) into Equation (4.1) gives

$$L(\alpha,\beta)=\prod_{i=1}^{n}\left(\frac{\alpha}{x_i\left[\ln(x_i)\right]^2}\mathrm{e}^{-\frac{\alpha}{\beta}\left(e^{-\frac{\beta}{\ln(x_i)}}-1\right)-\frac{\beta}{\ln(x_i)}}\right), \tag{4.2}$$

$$L(\alpha,\beta)=\alpha^n\prod_{i=1}^{n}\left(\frac{1}{x_i\left[\ln(x_i)\right]^2}\right)\exp\left[\sum_{i=1}^{n}\left(-\frac{\alpha}{\beta}e^{-\frac{\beta}{\ln(x_i)}}+\frac{\alpha}{\beta}-\frac{\beta}{\ln(x_i)}\right)\right], \tag{4.3}$$

the log-likelihood function is

$$\ell=n\ln(\alpha)-\sum_{i=1}^{n}\ln(x_i)-2\sum_{i=1}^{n}\ln\left[\ln(x_i)\right]+\sum_{i=1}^{n}\left(-\frac{\alpha}{\beta}e^{-\frac{\beta}{\ln(x_i)}}+\frac{\alpha}{\beta}-\frac{\beta}{\ln(x_i)}\right), \tag{4.4}$$

differentiating Equation (4.4) partially for α and β gives

$$\frac{\ell}{\partial\alpha}=\frac{n}{\alpha}-\sum_{i=1}^{n}\left(\frac{1}{\beta}e^{-\frac{\beta}{\ln(x_i)}}+\frac{1}{\beta}\right), \tag{4.5}$$

and

$$\frac{\ell}{\partial\beta}=\sum_{i=1}^{n}\left(\frac{\alpha}{\beta^2}e^{-\frac{\beta}{\ln(x_i)}}+\frac{\alpha}{\beta}\frac{e^{-\frac{\beta}{\ln(x_i)}}}{\ln(x_i)}-\frac{\alpha}{\beta^2}-\frac{1}{\ln(x_i)}\right) \tag{4.6}$$

respectively. Equating Equations (4.5) and (4.6) each to zero, gives

$$\frac{n}{\alpha}-\frac{1}{\beta}\sum_{i=1}^{n}e^{-\frac{\beta}{\ln(x_i)}}+\frac{n}{\beta}=0; \tag{4.7}$$

$$\frac{\alpha}{\beta^2}\sum_{i=1}^{n}e^{-\frac{\beta}{\ln(x_i)}}+\frac{\alpha}{\beta}\sum_{i=1}^{n}\frac{e^{-\frac{\beta}{\ln(x_i)}}}{\ln(x_i)}-\frac{\alpha n}{\beta^2}-\sum_{i=1}^{n}\frac{n}{\ln(x_i)}=0 \tag{4.8}$$

solving Equations (4.7) and (4.8) simultaneously gives $\hat{\alpha}_{MLE}$ and $\hat{\beta}_{MLE}$ However, it requires the use of numerical optimization techniques via the aid of software such as *R* or Python (Nash, [34]).

4.2. Maximum Product of Spacing (MPS) Estimation

The MPS is obtained by minimizing the function

$$m(\alpha,\beta)=\frac{1}{n+1}\sum_{i=1}^{n+1}\ln\left[F(x_{(i)};\alpha,\beta)-F(x_{(i-1)};\alpha,\beta)\right]. \tag{4.9}$$

Let $F(X_{(i)})$ be the cdf of order statistics $x_{(1)}\leq x_{(2)}\leq\ldots\leq x_{(n)}$, from $LIGD(\alpha,\beta)$. Therefore, the ith order statistic for $F(X_{(i)};\alpha,\beta)$ and $F(X_{(i-1)};\alpha,\beta)$ is expressed respectively as

$$F(x_{(i)};\alpha,\beta)=1-\exp\left[-\frac{\alpha}{\beta}\left(e^{-\frac{\beta}{\ln(x_{(i)})}}-1\right)\right], \tag{4.10}$$

and

$$F(x_{(i-1)};\alpha,\beta) = 1 - \exp\left[-\frac{\alpha}{\beta}\left(e^{-\frac{\beta}{\ln(x_{(i-1)})}} - 1\right)\right] \tag{4.11}$$

substituting Equations (4.10) and (4.11) into (4.9) gives

$$m = \frac{1}{n+1}\sum_{i=1}^{n+1} \ln\left[e^{-\frac{\alpha}{\beta}\left(e^{-\frac{\beta}{\ln(x_{(i-1)})}}-1\right)} - e^{-\frac{\alpha}{\beta}\left(e^{-\frac{\beta}{\ln(x_{(i)})}}-1\right)}\right], \tag{4.12}$$

The partial derivative of Equation (4.12) with respect to α and β gives

$$\frac{\partial m}{\partial \alpha} = \frac{1}{n+1}\cdot\frac{1}{\beta}\cdot\sum_{i=1}^{n+1}\frac{1}{D_i(\alpha,\beta)}\left[\left(e^{-\frac{\beta}{\ln(x_{(i)})}}-1\right)e^{-\frac{\left(e^{-\frac{\beta}{\ln(x_{(i)})}}-1\right)^{\alpha}}{\beta}} - \left(e^{-\frac{\beta}{\ln(x_{(i-1)})}}-1\right)e^{-\frac{\left(e^{-\frac{\beta}{\ln(x_{(i-1)})}}-1\right)^{\alpha}}{\beta}}\right] \tag{4.13}$$

and

$$\frac{\partial m}{\partial \beta} = \frac{1}{n+1}\cdot\frac{\alpha}{\beta^2}\cdot\sum_{i=1}^{n+1}\frac{1}{D_i(\alpha,\beta)}\left[\left(1-e^{-\frac{\beta}{\ln(x_{(i)})}} - \frac{\beta e^{-\frac{\beta}{\ln(x_{(i)})}}}{\ln(x_{(i)})}\right)e^{-\frac{\alpha\left(e^{-\frac{\beta}{\ln(x_{(i)})}}-1\right)}{\beta}} - \left(1-e^{-\frac{\beta}{\ln(x_{(i-1)})}} - \frac{\beta e^{-\frac{\beta}{\ln(x_{(i-1)})}}}{\ln(x_{(i-1)})}\right)e^{-\frac{\alpha\left(e^{-\frac{\beta}{\ln(x_{(i-1)})}}-1\right)}{\beta}}\right] \tag{4.14}$$

respectively, where $D_i(\alpha,\beta) = F(X_{(i)};\alpha,\beta) - F(X_{(i-1)};\alpha,\beta)$, $i = 1,2,...,n+1$.
Solving the system of Equations (4.13) and (4.14) has to be done numerically in order to obtain the estimates $\hat{\alpha}_{MPS}$ and $\hat{\beta}_{MPS}$.

5. Simulation Study

Here, the performance and the consistency of the MLE and MPS of the parameters of LIGD are assessed. Three different sets of metrics were considered, and a simulation with 10000 replications was used to generate samples of varying sizes from the LIGD.All simulations were run using R language of the optim function and the L-BFGS-B method. The simulation results compared the actual parameter values with the estimates. The performance of these estimators is assessed using mean estimates, bias, mean square error (MSE) and mean relative error (MRE) for each case. The simulation results are given in Tables 1 - 4.

Table 1. The Simulation results of LIGD for $\alpha = 0.825, \beta = 0.217$

		MLE				**MPS**			
n	Par.	Mean	Bias	MSE	MRE	Mean	Bias	MSE	MRE
25	α	0.845	0.020	0.063	0.024	0.933	0.108	0.085	0.131
	β	0.320	0.103	0.098	0.474	0.114	-0.103	0.085	0.476
50	α	0.841	0.016	0.030	0.019	0.893	0.068	0.037	0.082
	β	0.267	0.050	0.040	0.228	0.145	-0.072	0.037	0.332
150	α	0.840	0.015	0.010	0.018	0.865	0.040	0.012	0.048
	β	0.225	0.008	0.015	0.037	0.222	0.007	0.014	0.033
350	α	0.836	0.011	0.004	0.014	0.849	0.024	0.005	0.030
	β	0.217	0.000	0.003	0.001	0.189	-0.028	0.008	0.125
500	α	0.834	0.009	0.003	0.011	0.842	0.017	0.004	0.021
	β	0.217	0.000	0.003	0.001	0.194	-0.023	0.003	0.105

Table 2. The Simulation results of LIGD for $\alpha = 0.371, \beta = 1.465$

		MLE				**MPS**			
n	Par.	Mean	Bias	MSE	MRE	Mean	Bias	MSE	MRE
25	α	0.423	0.052	0.031	0.139	0.512	0.141	0.057	0.379
	β	1.609	0.145	0.239	0.098	1.338	-0.127	0.087	0.087
50	α	0.406	0.035	0.014	0.094	0.459	0.088	0.035	0.237
	β	1.484	0.015	0.053	0.037	1.377	-0.092	0.037	0.067
150	α	0.394	0.023	0.005	0.061	0.417	0.046	0.007	0.125
	β	1.847	0.382	0.105	0.213	1.640	0.028	0.018	0.019
350	α	0.387	0.016	0.002	0.042	0.389	0.019	0.002	0.051
	β	1.398	-0.067	0.009	0.048	1.405	-0.048	0.007	0.035
500	α	0.386	0.015	0.002	0.039	0.391	0.020	0.002	0.054
	β	1.468	0.083	0.009	0.062	1.439	-0.026	0.010	0.018

Table 3. The Simulation results of LIGD for $\alpha = 0.087, \beta = 4.505$

		MLE				**MPS**			
n	Par.	Mean	Bias	MSE	MRE	Mean	Bias	MSE	MRE
25	α	0.106	0.019	0.004	0.219	0.143	0.056	0.010	0.648
	β	4.710	0.205	0.115	0.046	4.238	-0.267	0.271	0.059
50	α	0.097	0.010	0.002	0.119	0.119	0.032	0.003	0.366
	β	4.643	0.133	0.070	0.031	4.341	-0.161	0.231	0.037
150	α	0.094	0.007	0.001	0.075	0.105	0.018	0.001	0.175
	β	4.591	0.086	0.038	0.019	4.469	-0.022	0.016	0.005
350	α	0.091	0.004	0.000	0.049	0.094	0.006	0.000	0.098
	β	4.517	0.012	0.016	0.003	4.487	-0.018	0.004	0.002
500	α	0.091	0.004	0.000	0.044	0.094	0.007	0.000	0.082
	β	4.509	0.004	0.034	0.001	4.509	0.000	0.000	0.000

Table 4. The Simulation results of LIGD for $\alpha = 0.131, \beta = 9.018$

		MLE				MPS			
n	Par.	Mean	Bias	MSE	MRE	Mean	Bias	MSE	MRE
25	α	0.163	0.032	0.011	0.225	0.222	0.091	0.025	0.592
	β	9.417	0.419	2.799	0.047	8.943	-0.075	0.692	0.008
50	α	0.146	0.015	0.005	0.115	0.182	0.051	0.009	0.390
	β	9.203	0.185	0.815	0.020	8.652	-0.366	0.229	0.042
150	α	0.138	0.007	0.001	0.052	0.150	0.019	0.002	0.141
	β	9.029	0.011	0.139	0.001	9.110	0.092	0.014	0.010
350	α	0.130	-0.001	0.000	0.010	0.134	0.003	0.000	0.021
	β	9.011	-0.007	0.120	0.001	8.987	-0.031	0.006	0.003
500	α	0.129	-0.002	0.000	0.012	0.132	0.001	0.000	0.007
	β	9.028	0.010	0.109	0.001	8.929	-0.089	0.004	0.010

Tables 1 - 4 show the simulation results comparing the performance of MLE and MPS under three different metrics combinations with increasing sample sizes. According to both methods of estimation, it is evident that as sample size increases, the average estimates tend towards the true parameter values. Also, the biases, MSEs, and MREs converge towards zero as the sample size increases. However, the MLE has smaller bias, MSE, and MRE compared to MPS across all parameter combinations and sample sizes. Hence, MLE is the preferred technique for estimating the parameters of the LIGD. If researchers have data that matches the proposed model, it is recommended that they use this technique.

6. Applications

This section presents LIGD's applicability to two real datasets in comparison to other competing distributions. The competing distributions used in this study are those from generalized IGDs, log-modified and unit-bounded distributions; and are specified in Table 5.

Table 5. List of the competing distributions

Distribution	Abbreviation	Author(s)
Topp-Leone Inverse Gompertz	TLIGD	Adegoke et al. [19]
Half-Cauchy Inverse Gompertz	HCIGD	Chaudhary et al. [17]
Kumaraswamy Inverse Gompertz	KuIGD	El-Morshedy et al. [14]
Inverse Power Gompertz	PIGD	Abdelhady and Amer [15]
Inverse Gompertz	IGD	Eliwa et al. [13]
Log-Logistics	LLoD	Muse et al. [35]
Log-Kumaraswamy	LKuD	Ishaq et al. [36]
Log-Normal	LNoD	Limpert et al. [37]
Log-Cauchy	LCaD	Ali and Habibullah [38]
Kumaraswamy	KuD	Sultana et al. [39]
Beta	BeD	Johnson et al. [40]
Unit Burr-XII	UBXII	Korkmaz and Chesneau [1]
Unit Weibull	UWeD	Mazucheli et al. [2]
Unit Teissier	UTeD	Krishna et al. [41]
Rayleigh	URaD	Bantan et al. [42]

To select the best model, the discrimination criteria ($-\hat{\ell}$, AIC, CAIC, BIC and HQIC) and goodness-of-fit test (KS statistic with its associated p-value) are considered. The model with the smallest discrimination criteria values is said to have outperformed the other competitors in modelling the data.

Similarly, the model with the smallest goodness-of-fit statistics provides the superior fit. A low p-value (< 0.05) indicates that the model does not fit the data, while a high p-value (≥ 0.05) suggests that the model is a good fit for the data (Kar and Mohanty, [43]). The values of the MLEs of the fitted models along with the above statistical measures were computed using the optimization package AdequacyModel in R-script with optim() and method=SANN (Marinho et al. [44]).

6.1. Data Source and Descriptive Analysis

The first dataset is the insurance data (Afify et al. [45]), sourced from the U.S. government's open-data portal, and comprises 58 observations of claim ratios which are
0.188, 0.202, 0.195, 0.385, 0.489, 0.545, 0.541, 0.535, 0.521, 0.508, 0.512, 0.507, 0.519, 0.493, 0.487, 0.460, 0.490, 0.460, 0.490, 0.500, 0.400, 0.350, 0.370, 0.410, 0.400, 0.400, 0.410, 0.400, 0.420, 0.450, 0.450, 0.420, 0.390, 0.340, 0.360, 0.400, 0.440, 0.390, 0.410, 0.450, 0.460, 0.470, 0.490, 0.460, 0.410, 0.390, 0.400, 0.440, 0.420, 0.420, 0.450, 0.470, 0.530, 0.420, 0.490, 0.440, 0.420, 0.400.
The second dataset represents soil moisture reported by Maiti and Maity [46]. Soil moisture data often exhibits low noise, that is, fewer samples are needed to detect trends (Vereecken et al. [47]). The dataset is given as
0.0179, 0.0798, 0.0959, 0.0444, 0.0938, 0.0443, 0.0917, 0.0882, 0.0439, 0.0490, 0.0774, 0.0171, 0.0305, 0.0757, 0.0468.

The descriptive statistics of these datasets are supplied in Table 6.

Table 6. Summary of the datasets.

Data	n	Min	Med	Mode	Mean	Max	Std Dev	Skewness	Kurtosis
Insurance	58	0.1880	0.4400	0.4000	0.4322	0.5450	0.0754	-1.3754	5.8260
Soil Moisture	15	0.0171	0.0490	0.0171	0.0598	0.0959	0.1634	-0.1083	1.6247

The histograms for the datasets are shown in Figure 4, respectively. It clearly shows that the data are both left skewed.

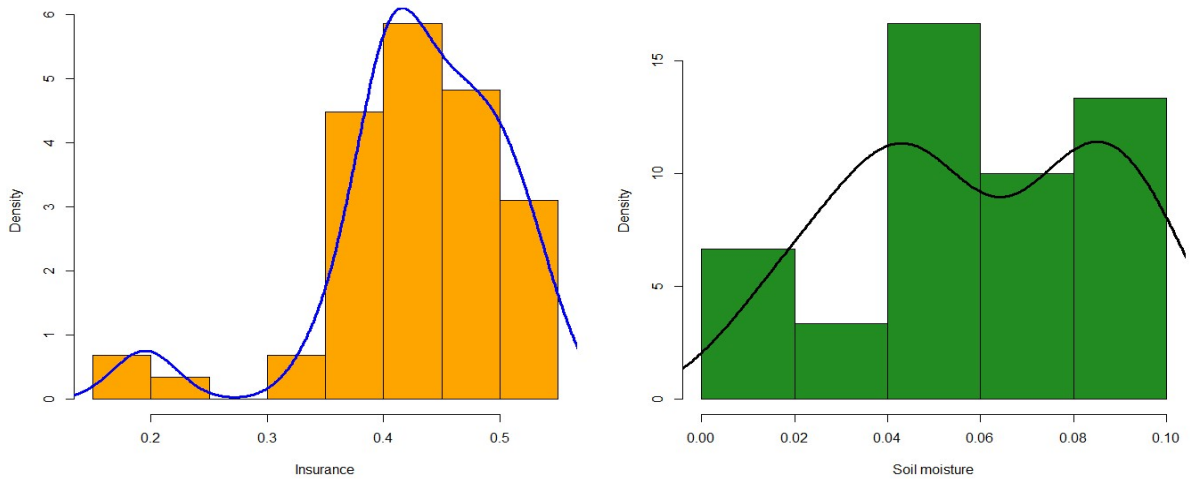

Figure 4. Histogram of insurance and soil moisture datasets.

6.2. *Analytical Results of Competing Models of the Insurance Data*

The MLEs, and other performance measures of LIGD with other competing models of the insurance data are tabulated in Tables 7 - 9 respectively.

Table 7. Performance of the LIGD against competing generalized IGDs using first dataset.

Models	**MLEs**	$\hat{\ell}$	**AIC**	**BIC**	**KS**	**KS** (p-**value**)
LIGD	$\hat{\alpha} = 0.007, \hat{\beta} = 4.954$	-33.122	-62.245	-60.829	0.168	0.731
TLIGD	$\hat{a} = 0.774, \hat{b} = 0.008, \hat{c} = 0.069$	-29.906	-53.812	-51.688	0.224	0.383
HCIGD	$\hat{a} = 0.085, \hat{b} = 4.024, \hat{c} = 0.088$	-29.620	-53.240	-51.116	0.225	0.377
KuIGD	$\hat{a} = 0.172, \hat{b} = -0.024, \hat{c} = 8.001$	-31.983	-57.965	-55.841	0.177	0.673
PIGD	$\hat{a} = 0.015, \hat{b} = 0.005, \hat{c} = 1.205$	-28.284	-50.568	-48.443	0.288	0.135
IGD	$\hat{a} = 0.031, \hat{b} = 0.021$	-27.903	-51.806	-50.390	0.306	0.096

Table 8. Performance of the LIGD against competing log-modified models using first dataset.

Models	**MLEs**	$\hat{\ell}$	**AIC**	**BIC**	**KS**	**KS** (p-**value**)
LIGD	$\hat{\alpha} = 0.007, \hat{\beta} = 4.954$	-73.752	-143.505	-139.384	0.129	0.291
LNoD	$\hat{a} = -0.859, \hat{b} = 0.212$	-56.943	-109.885	-105.764	0.211	0.011
LLoD	$\hat{a} = 0.436, \hat{b} = 10.403$	-66.056	-128.113	-123.992	0.102	0.587
LCaD	$\hat{a} = -0.827, \hat{b} = 0.090$	-66.164	-128.327	-124.206	0.124	0.336
LKuD	$\hat{a} = 3.901, \hat{b} = 45.110$	-48.247	-92.495	-88.374	0.290	< 0.0001

Table 9. Performance of the LIGD against competing unit-bounded models using first dataset

Models	**MLEs**	$\hat{\ell}$	**AIC**	**BIC**	**KS**	**KS** (p-**value**)
LIGD	$\hat{\alpha} = 0.007, \hat{\beta} = 4.954$	-73.752	-143.505	-139.384	0.129	0.291
KuD	$\hat{a} = 4.627, \hat{b} = 34.034$	-64.084	-124.167	-120.047	0.218	0.008
Beta	$\hat{a} = 16.201, \hat{b} = 21.363$	-65.506	-127.011	-122.890	0.172	0.066
UBXII	$\hat{a} = 2.250, \hat{b} = 6.273$	-65.432	-126.864	-122.743	0.171	0.068
URaD	$\hat{a} = 1.277$	-35.935	-69.869	-67.809	0.375	< 0.0001
UWeD	$\hat{a} = 1.243, \hat{b} = 3.625$	-52.035	-100.070	-95.949	0.230	0.004
UTeD	$\hat{a} = 1.274$	-42.405	-82.811	-82.750	0.325	< 0.0001

As observed in Tables 7 - 9, the LIGD has the smallest information criteria than its competitors, thus, the LIGD outperforms all other competing models and A* values than other competing models, hence, LIGD outperforms all the competing models. Also, the LIGD has the smaller KS value and a KS p-value (0.291) which is ≥ 0.05, thus, the LIGD provides a better fit for the insurance data. However, LLoD and LCaD provide the best fit compared to the LIGD. This conclusion is further supported by the histogram of the insurance data alongside the densities and Quantile-Quantile (QQ) plots for all the fitted distributions shown in Figures 5 and 6.

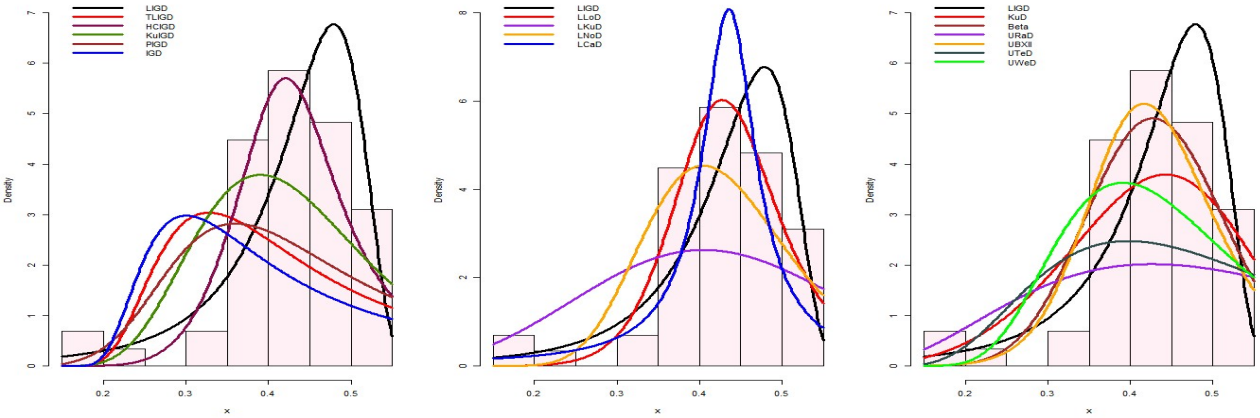

Figure 5. The estimated pdfs for insurance data.

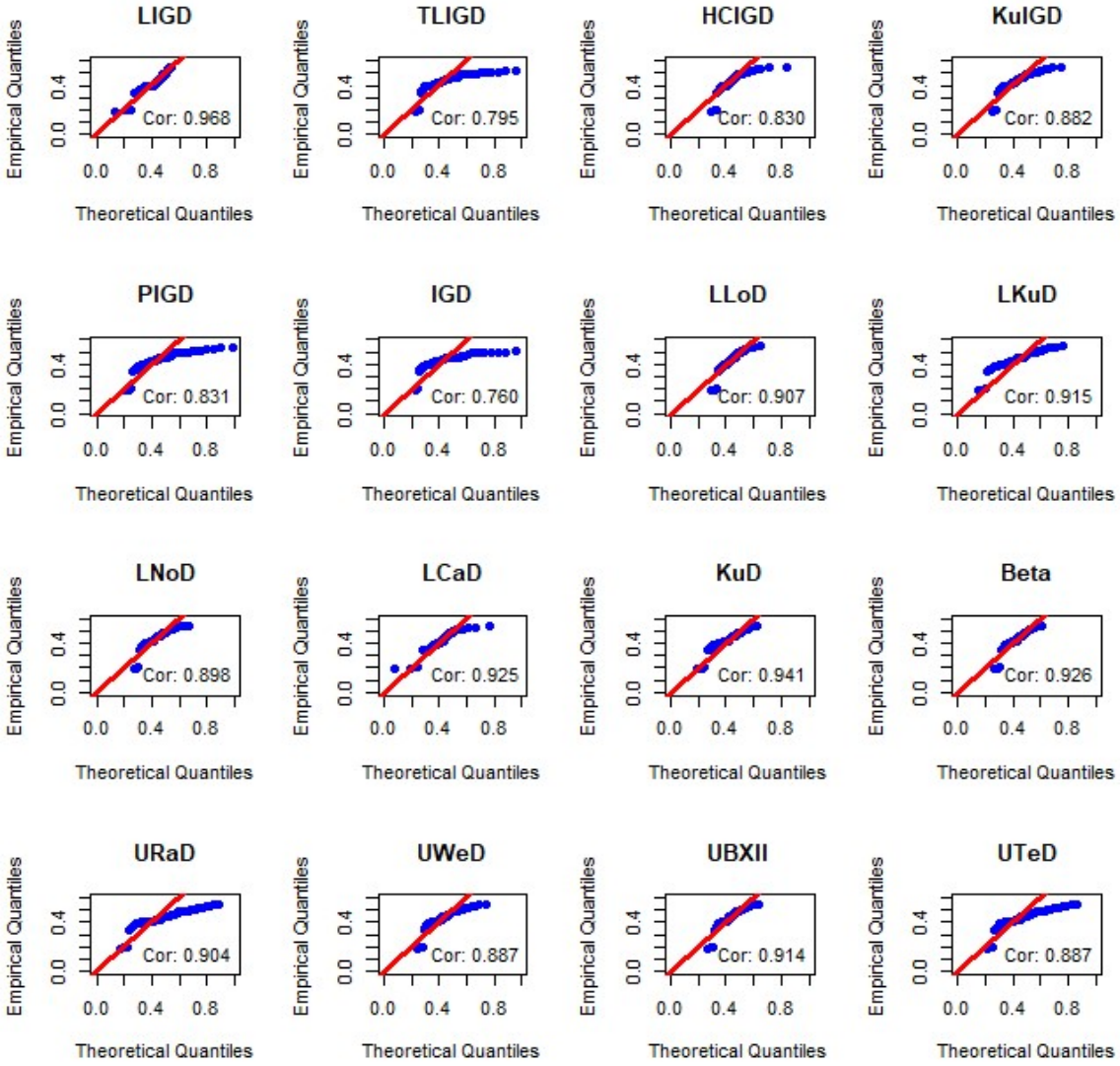

Figure 6. The QQ plots for insurance data.

Figure 5 shows that the LIGD distribution offers a close fit to the insurance data. Similarly, as illustrated in Figure 6, distributions such as LCaD, KuD, and Beta also exhibit strong correlation with the data, as evidenced by their high correlation coefficients (0.925, 0.941, and 0.926, respectively). In particular, the LIGD achieves the highest correlation coefficient (0.968), which highlights its superior performance. Taken together, these graphical analyzes substantiate the robustness and superiority of LIGD in modeling the insurance data set.

6.3. Analytical Results of Competing Models of Soil Moisture Data

The MLEs, and other performance measures of LIGD with other competing models of the soil moisture data are tabulated in Tables 10 - 12 respectively.

Table 10. Performance of the LIGD against competing generalized IGDs using second dataset.

Models	**MLEs**	$\hat{\ell}$	**AIC**	**BIC**	**KS**	**KS** (p-**value**)
LIGD	$\hat{\alpha} = 0.039, \hat{\beta} = 16.002$	-33.122	-62.245	-60.829	0.168	0.731
TLIGD	$\hat{a} = 0.774, \hat{b} = 0.008, \hat{c} = 0.069$	-29.906	-53.812	-51.688	0.224	0.383
HCIGD	$\hat{a} = 0.085, \hat{b} = 4.024, \hat{c} = 0.088$	-29.620	-53.240	-51.116	0.225	0.377
KuIGD	$\hat{a} = 0.172, \hat{b} = -0.024, \hat{c} = 8.001$	-31.983	-57.965	-55.841	0.177	0.673
PIGD	$\hat{a} = 0.015, \hat{b} = 0.005, \hat{c} = 1.205$	-28.284	-50.568	-48.443	0.288	0.135
IGD	$\hat{a} = 0.031, \hat{b} = 0.021$	-27.903	-51.806	-50.390	0.306	0.096

Table 11. Performance of the LIGD against competing log-modified models using second dataset.

Models	**MLEs**	$\hat{\ell}$	**AIC**	**BIC**	**KS**	**KS** (p-**value**)
LIGD	$\hat{\alpha} = 0.039, \hat{\beta} = 16.002$	-33.122	-62.245	-60.829	0.168	0.731
LNoD	$\hat{a} = -2.953, \hat{b} = 0.550$	-31.862	-59.724	-58.308	0.217	0.419
LLoD	$\hat{a} = 0.056, \hat{b} = 3.160$	-31.609	-59.217	-57.801	0.191	0.580
LCaD	$\hat{a} = -2.802, \hat{b} = 0.377$	-28.694	-53.388	-51.971	0.219	0.407
LKuD	$\hat{a} = 1.282, \hat{b} = 29.780$	-29.398	-54.797	-53.381	0.242	0.296

Table 12. Performance of the LIGD against competing unit-bounded models using second dataset.

Models	**MLEs**	$\hat{\ell}$	**AIC**	**BIC**	**KS**	**KS** (p-**value**)
LIGD	$\hat{\alpha} = 0.039, \hat{\beta} = 16.002$	-33.122	-62.245	-60.829	0.168	0.731
KuD	$\hat{a} = 1.241, \hat{b} = 25.552$	-29.442	-54.885	-53.469	0.239	0.307
Beta	$\hat{a} = 1.951, \hat{b} = 27.524$	-31.088	-58.176	-56.760	0.217	0.421
UBXII	$\hat{a} = 0.104, \hat{b} = 9.008$	-12.305	-20.609	-19.193	0.548	< 0.0001
URaD	$\hat{a} = 1.111$	-22.633	-43.266	-42.558	0.457	0.002
UWeD	$\hat{a} = 0.002, \hat{b} = 5.314$	-30.971	-57.943	-56.526	0.194	0.559
UTeD	$\hat{a} = 0.387$	-25.126	-48.253	-47.545	0.436	0.004

As shown in Tables 10 - 12, the LIGD outperforms its competing models with the lowest information criteria. In addition, the LIGD has the smallest KS values and the highest KS p-value (0.731), confirming its superior fit. This conclusion is further supported by the soil moisture data histogram alongside the densities and QQ plots for all the fitted distributions shown in Figures 7 and 8.

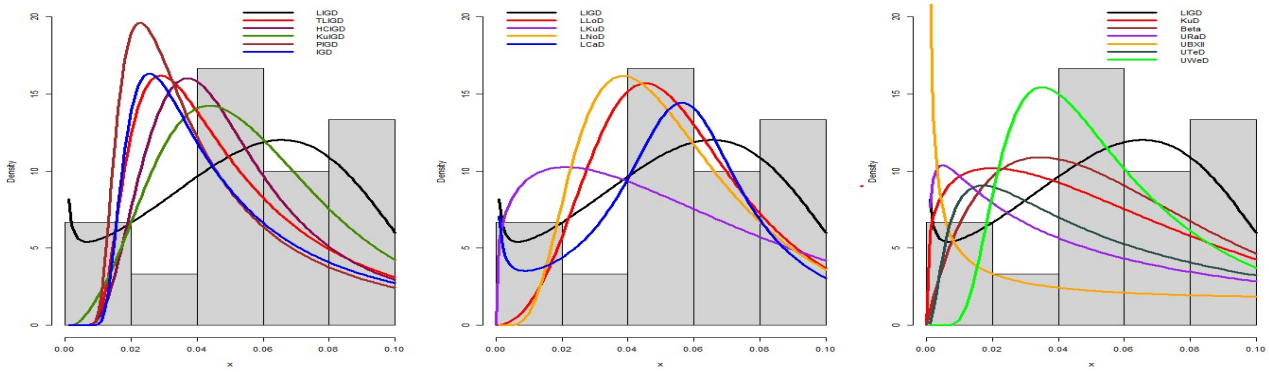

Figure 7. The estimated pdfs for soil moisture data.

Figure 7 demonstrates that the LIGD distribution offers a close fit to the soil moisture data. Similarly, as illustrated in Figure 8, distributions such as KuD, Beta, and UBXII also exhibit strong correlation with the data, as evidenced by their high correlation coefficients (0.928, 0.934, and 0.950, respectively). Notably, the LIGD achieves the highest correlation coefficient (0.972), underscoring its superior performance. Collectively, these graphical analyses substantiate the LIGD's robustness and superiority in modeling the soil moisture dataset.

7. Conclusion

This study introduced a novel two-parameter distribution, termed the Log Inverse Gompertz Distribution (LIGD), as an extension of the Inverse Gompertz distribution for modeling data restricted to the unit interval (0, 1). The LIGD was derived through a negative exponential transformation of the inverse Gompertz distribution. Its probability density function displayed unimodal behavior and accommodated a variety of shapes, including J-shaped and reversed-J forms, while its hazard rate function exhibited a monotonically increasing pattern. Some statistical properties and reliability measures were derived, highlighting the distribution's applicability in practical data analysis. Parameter estimation was carried out using the methods of maximum likelihood and maximum product of spacing, with a Monte Carlo simulation study conducted to evaluate the estimators' performance. The application of the new model to insurance and soil moisture datasets revealed its superior fit over competing models, reinforcing its effectiveness for analyzing unit-bounded data.

Funding Statement: This work was supported and funded by the Deanship of Scientific Research at Imam Mohammad Ibn Saud Islamic University (IMSIU) (grant number IMSIU-DDRSP2504).
Acknowledgments: This work was supported and funded by the Deanship of Scientific Research at Imam Mohammad Ibn Saud Islamic University (IMSIU) (grant number IMSIU-DDRSP2504).
Conflict of Interest: The authors declare no conflict of interest.
Data availability Statement: Data is available from the corresponding authors upon reasonable re-

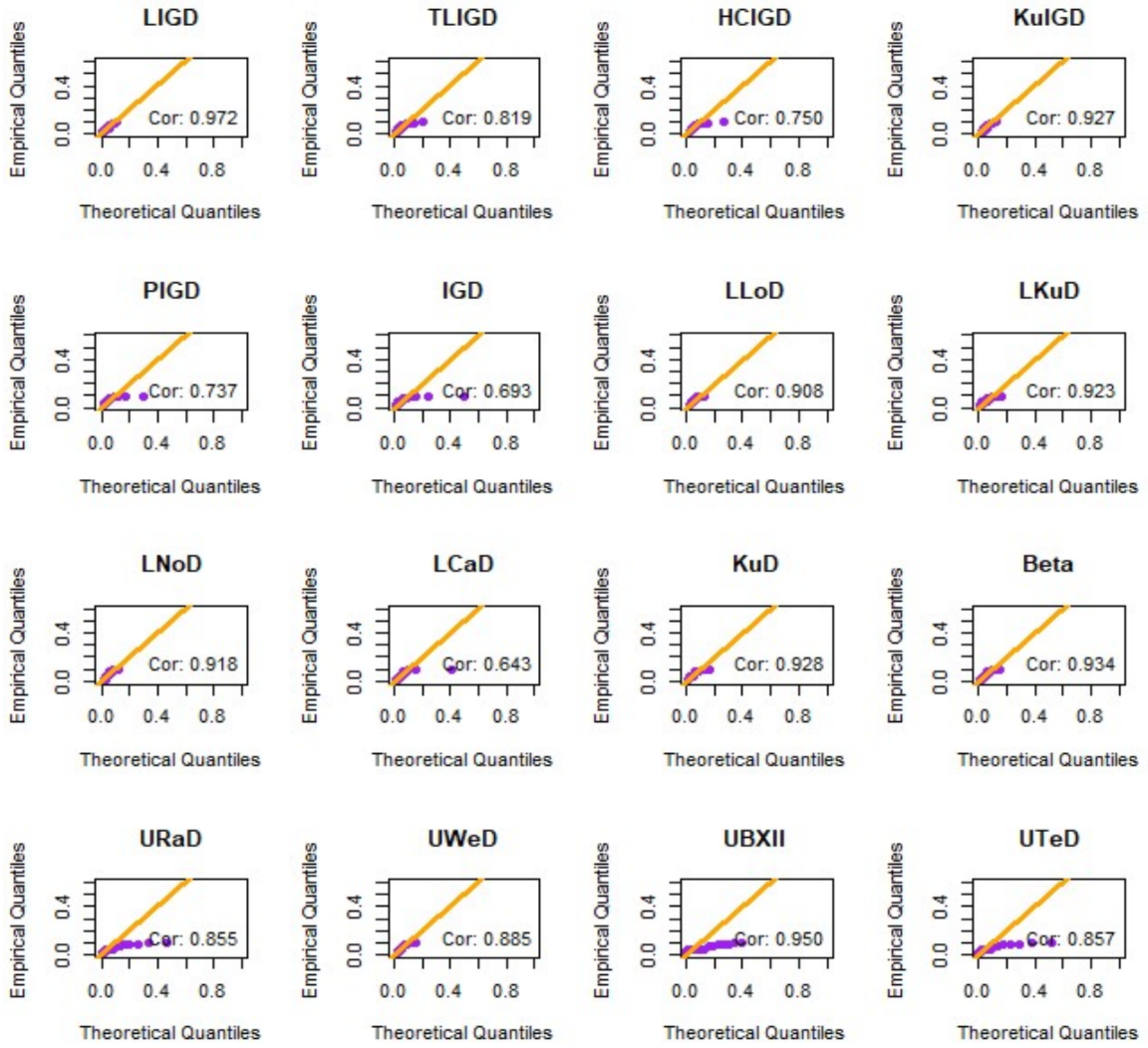

Figure 8. The QQ Plots for soil moisture data.

quest.

References

1. Korkmaz, M. Ç., Chesneau, C., and Korkmaz, Z. S. (2021). Transmuted unit Rayleigh quantile regression model: Alternative to beta and Kumaraswamy quantile regression models. Univ. Politeh. Buchar. Sci. Bull. Ser. Appl. Math. Phys, 83, 149-158.
2. Mazucheli, J., Menezes, A. F., and Dey, S. (2019). Unit-Gompertz distribution with applications. Statistica, 79(1), 25-43.
3. Altun, E. and Cordeiro, G. M. (2020). The unit-improved second-degree Lindley distribution: inference and regression modeling. Computational Statistics, 35(1), 259–279.
4. Bashir, S., Masood, B., Al-Essa, L. A., Sanaullah, A., and Saleem, I. (2024). Properties, Quantile Regression, and Application of Bounded Exponentiated Weibull distribution to COVID-19 Data of Mortality and Survival Rates. Scientific Reports, 14(1), 1-17.

5. Saboor, A. ., Jamal , F., Shafq, S. ., & Mumtaz, R. . (2025). On the Versatility of the Unit Logistic Exponential Distribution: CapturingBathtub, Upside-Down Bathtub, and Monotonic Hazard Rates. Innovation in Statistics and Probability , 1(1), 28-46.

6. Gemeay, A. M., Alsadat, N., Chesneau, C., & Elgarhy, M. (2024). Power unit inverse Lindley distribution with different measures of uncertainty, estimation and applications. AIMS Mathematics, 9(8), 20976-21024.

7. Alghamdi, S. M., Shrahili, M., Hassan, A. S., Mohamed, R. E., Elbatal, I., & Elgarhy, M. (2023). Analysis of milk production and failure data: using unit exponentiated half logistic power series class of distributions. Symmetry, 15(3), 714.

8. Alsadat, N., Elgarhy, M., Karakaya, K., Gemeay, A. M., Chesneau, C., & Abd El-Raouf, M. M. (2023). Inverse unit Teissier distribution: Theory and practical examples. Axioms, 12(5), 502.

9. Haj Ahmad, H., Almetwally, E. M., Elgarhy, M., & Ramadan, D. A. (2023). On unit exponential Pareto distribution for modeling the recovery rate of COVID-19. Processes, 11(1), 232.

10. Alyami, S. A., Elbatal, I., Alotaibi, N., Almetwally, E. M., & Elgarhy, M. (2022). Modeling to factor productivity of the United Kingdom food chain: Using a new lifetime-generated family of distributions. Sustainability, 14(14), 8942.

11. Jha, M. K., Dey, S., Alotaibi, R. M., and Tripathi, Y. M. (2020). Reliability estimation of a multi-component stress-strength model for unit Gompertz distribution under progressive type-II censoring. Quality and Reliability Engineering International, 36(4), 965-987.

12. Pandey, A., Bhushan, S., and Ralte, L. (2020). A mixture shared gamma frailty model under Gompertz baseline distribution. Journal of the Indian Society for Probability and Statistics, 21(2), 187-203.

13. Eliwa, M. S., El-Morshedy, M., and Ibrahim, M. (2019). Inverse Gompertz distribution: properties and different estimation methods with application to complete and censored data. Annals of data science, 6, 321-339.

14. El-Morshedy, M., El-Faheem, A. A., Al-Bossly, A., and El-Dawoody, M. (2021). Exponentiated generalized inverted gompertz distribution: Properties and estimation methods with applications to symmetric and asymmetric data. Symmetry, 13(10), 1868.

15. Abdelhady, D. H., and Amer, Y. M. (2021). On the inverse power Gompertz distribution. Annals of Data Science, 8(3), 451-473.

16. Elshahhat, A., Aljohani, H. M., and Afify, A. Z. (2021). Bayesian and classical inference under Type-II censored samples of the extended inverse Gompertz distribution with engineering applications. Entropy, 23(12), 1578.

17. Chaudhary, A. K., Yadav, R. S., and Kumar, V. (2022). Half-Cauchy Inverse Gompertz Distribution: Theory and Applications. International Journal of Statistics and Applied Mathematics, 7(5),: 94-102.

18. Abd Ellatif, E. M., and Abd Ellatif, S. M. (2022). Marshall–Olkin Inverse Gompertz distribution with reliability applications. Reliability Engineering & System Safety, 220, 108282.

19. Adegoke, T. M., Abimbola, L. A., Oladoja, O. M., Oyebanjo, O. R., and Obisesan, K. O. (2024). Bayesian Estimation of Parameters and Reliability Characteristics in the Inverse Gompertz Distribution. Reliability: Theory and Applications, 19(3), 744-756.

20. Baharith, L.A. (2024). New Generalized Weibull Inverse Gompertz Distribution: Properties and Applications. Symmetry, 2024, 16, 197.

21. Benkhelifa, L. (2017). The Marshall–Olkin Extended Generalized Gompertz Distribution. Journal of Data Science, 15(2), 239–266.

22. Yadav, R. S., and Kumar, V. (2023). Exponentiated Inverse Gompertz distribution and its applications in reliability. Communications in Statistics- Theory and Methods, 52(3), 781–799.

23. Al-Saqal, O. E., Hadied, Z. A., and Algamal, Z. Y. (2025). Modelling bladder cancer survival function based on neutrosophic inverse Gompertz distribution. International Journal of Neutrosophic Science (IJNS), 25(1), 75-80.

24. Alzaatreh, A., Famoye, F., and Lee, C. (2014). The Gamma-Normal Distribution: Properties and Applications. Computational Statistics and Data Analysis, 69, 67–80.

25. Suleiman, A. A., Daud, H., Usman, A. G., Abba, S. A., Othman, M and M. Elgarhy (2025). A new two parameters half-logistic distribution with numerical analysis and application. Journal of Statistical Sciences and Computational Intelligence, 1(1), 1–28.

26. Uthumporn, P., Ishaq, A. I., Usman, A., Sadiq, I. A. and Mohammed, A. S. (2025). The modified sine distribution and machine learning models for enhancing crude oil production prediction. Journal of Statistical Sciences and Computational Intelligence, 1(1), 29–45.

27. Husain, Q. N. ., Qaddoori , A. S. ., Noori , N. A. ., Abdullah, K. N. ., Suleiman, A. A. ., and Balogun, O. S. . (2025). New Expansion of Chen Distribution According to the Nitrosophic Logic Using the Gompertz Family. Innovation in Statistics and Probability , 1(1), 60-75.

28. Sapkota, L. P. ., Kumar, V. ., Tekle, G. ., Alrweili, H. ., Mustafa, M. S. ., & Yusuf, M. . (2025). Fitting Real Data Sets by a New Version of Gompertz Distribution. Modern Journal of Statistics, 1(1), 25-48.

29. Alsadat, N., Hassan, A. S., Elgarhy, M., Chesneau, C., & Mohamed, R. E. (2023). An efficient stress–strength reliability estimate of the unit Gompertz distribution using ranked set sampling. Symmetry, 15(5), 1121.

30. Bantan, R. A., Jamal, F., Chesneau, C., & Elgarhy, M. (2021). Theory and applications of the unit gamma/Gompertz distribution. Mathematics, 9(16), 1850.

31. Elbatal, I., Jamal, F., Chesneau, C., Elgarhy, M., & Alrajhi, S. (2018). The modified beta Gompertz distribution: theory and applications. Mathematics, 7(1), 3.

32. Bowley, L., 1901. Elements of Statistics, 6th ed. Staples Press Ltd., London, 1937.

33. Moors, J. J. A. (1988). A Quantile Alternative for Kurtosis. Journal of the Royal Statistical Society, Series D (The Statistician), 37(1), 25-32.

34. Nash, J. C. (2014). Nonlinear parameter optimization using R tools. John Wiley and Sons.

35. Muse, A. H., Mwalili, S. M., and Ngesa, O. (2021). On the log-logistic distribution and its generalizations: a survey. International Journal of Statistics and Probability, 10(3), 93-125.

36. Ishaq, A. I., Suleiman, A. A., Daud, H., Singh, N. S. S., Othman, M., Sokkalingam, R., and Abba, S. I. (2023). Log-Kumaraswamy distribution: its features and applications. Frontiers in Applied Mathematics and Statistics, 9, 1258961.

37. Limpert, E., Stahel, W. A., and Abbt, M. (2001). Log-normal Distributions across the Sciences: Keys and Clues. BioScience, 51(5), 341-352.

38. Ali, A., and Habibullah, S. N. (2016). On A Decile-Based SIA-Estimator of the Scale Parameter of the Log-Cauchy Distribution. In Proceedings of the 14th International Conference on Statistical Sciences, 29(1), 427-434.

39. Sultana, F., Tripathi, Y. M., Rastogi, M. K., and Wu, S. J. (2018). Parameter estimation for the Kumaraswamy distribution based on hybrid censoring. American Journal of Mathematical and Management Sciences, 37(3), 243-261.

40. Johnson, N. L., Kotz, S., and Balakrishnan, N. (1994). Beta distributions. Continuous univariate distributions, 2, 210-275.

41. Krishna, A., Maya, R., Chesneau, C., and Irshad, M. R. (2022). The Unit Teissier distribution and its applications. Mathematical and Computaional Applications 27(10), 1-20.

42. Bantan, R. A. R., Chesneau, C., Jamal, F., Elgarhy, M., Tahir, M. H., Ali, A., Zubair, M., and Anam, S. (2020). Some new facts about the unit-Rayleigh distribution with applications. Mathematics, 8(11), 1954.

43. Kar, C., and Mohanty, A. R. (2004). Application of KS test in ball bearing fault diagnosis. Journal of sound and vibration, 269(1-2), 439-454.

44. Marinho, P. R. D., Silva, R. B., Bourguignon, M., Cordeiro, G. M., and Nadarajah, S. (2019). AdequacyModel: An R package for Probability Distributions and General Purpose Optimization. PloS one, 14(8), e0221487.

45. Afify, A. Z., Gemeay, A. M., and Ibrahim, N. A. (2020). The Heavy-tailed Exponential Distribution: Risk Measures, Estimation, and Application to Actuarial Data. Mathematics, 8(8), 1276-1303.

46. Maiti, R., and Maity. (2018). Statistical methods in hydrology and hydroclimatology (Vol. 555). Singapore: Springer.

47. Vereecken, H., Schnepf, A., Hopmans, J.W., Javaux, M., Or, D., Roose, T., Vanderborght, J., Young, M.H., Amelung, W., Aitkenhead, M. and Allison, S.D. (2016). Modeling soil processes: Review, key challenges, and new perspectives. Vadose zone journal, 15(5), vzj2015-09.